POLITECNICO
MILANO 1863

SCUOLA DI INGEGNERIA INDUSTRIALE
E DELL'INFORMAZIONE

CFD Project - C_D assessment and pressure distribution for the VEGA launcher

Final Report for the project of the Computational Fluid Dynamics course

Group number Number of the group: 16

Enrico Barbiero, 10679931
Daniele Bossi, 10632967
Federico Cutolo, 10521274
Andrea De Meda, 10867580
Daniele Guernelli, 10504932

Lecturer:
Prof. Alberto Guardone

Tutor:
Prof. Giulio Gori

Abstract

In this report, the drag coefficient of a VEGA-like launcher at Mach number 1.99 is studied numerically. The solver used is SU2, while for the grid generation the software used is Gmsh. Two different grids (structured and unstructured) have been investigated and compared in terms of advantages and disadvantages (number of elements, accuracy of the result). A grid convergence has been carried out for the grids as verification of mesh-independent results. The numerical solution is obtained solving Euler equations with Roe scheme and a comparison between first and second order solution is presented. A thorough study of the pressure distribution along the surface is pursued to assess the drag coefficient. The numerical solution is then validated through the 2D steady Euler theory (oblique shocks relations and Prandtl-Meyer expansions) and the two are in excellent agreement. A grid optimization is investigated: by slightly varying the Mach number (1.85-2.5) for the same grid the results change within an acceptable range of error (lower than 0.85%).

1. Objectives

We hereby show the outline of our work. Despite it may look a neat, linear process, it's the result of a balance between the feasibility of the study with the available computational resources, and hence derived from a trial-and-error approach that affected the whole process multiple times.

- Geometry modeling (launcher)
- Problem modeling and methodology (hypothesis, equations, boundary conditions)
- Theoretical results
- Grid generation (structured and unstructured, features, convergence)
- Solver setup (scheme, parameters for convergence)
- Results and post-processing (RANS, validation, grids comparison, 1st-2nd order comparison, mach-varying, axi-alsymmetry comparison)

2. Geometry modeling

The geometry considered is inspired by the VEGA launcher development by the European Space Agency and Arianespace. An important requirement for this study was to have a comparison with experimental or theoretical data to validate it. To do so, while the geometry proportions are all met, we decided to simplify the geometry with straight lines. This allowed to have a direct connection of the pressure with the oblique-shock relations and Prandtl-Meyer expansion theory. This hypothesis deeply affects the flow around the rocket, as the expected bow shock at the nose is substituted with a cone-shock (or an oblique shock for the 2D case). And so happens for the aerodynamics along the body, where smooth curves are substituted with sharp corners, and so compression and expansion waves are concentrated in a single point at the surface. We will often call both shock and fan as *discontinuities* even though the latter is not a proper one, but it becomes one at the surface, where its characteristics meet at a single point. In addition, the bell-shaped nozzle in the rear part of the launcher is neglected. This simplification won't change the ahead aerodynamics, since for a supersonic inviscid flow the problem is hyperbolic and only *upwind* geometry modifications can affect it.
It was decided to use dimensional lengths, in order to have a more direct quantification of the discontinuities extension in the flow field. The body is 30 meters long, with a maximum radius of 1.5 m.

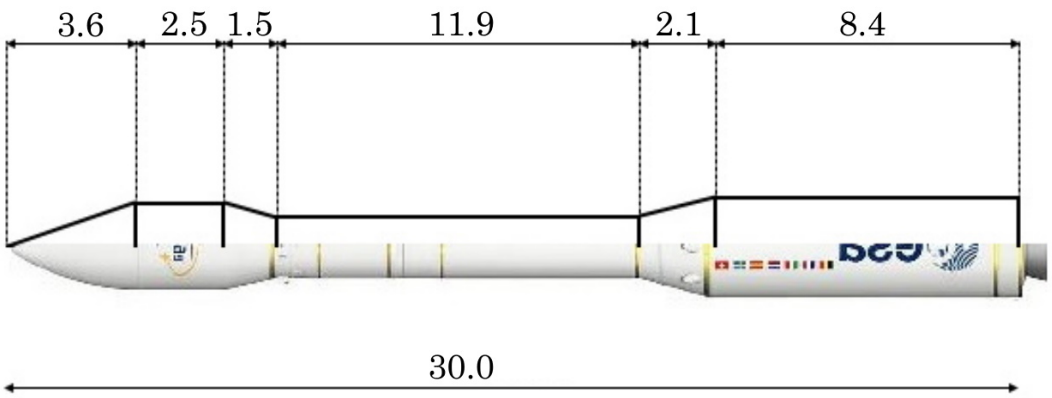

Figure 1: Vega vs Model

3. Problem modeling and methodology

We considered a 2D steady flow in supersonic conditions with the free-stream values taken at an altitude $h = 13000m$, at a speed $u = 587.207\frac{m}{s}$ [5] that, according to [1], corresponds to a Mach number $M = 1.99$, pressure $p = 16580Pa$, temperature $T = 216.66K$, density $\rho = 0.26659\frac{kg}{m^3}$. The angle of attack is set to zero, that stands for a vertical ascent of the launcher. Due to the high Reynolds number and the steadiness of the problem, it is adequate to describe the flow with the 2D-steady Euler equations, since the boundary layer is very thin and inertia forces prevail on the viscous ones. We considered the Euler problem and, subsequently, an attempt to solve the viscous case with the Reynolds-averaged Navier-Stokes' (RANS) equations was made; in the latter case, a thin boundary layer develops but the solution in the outer flow, as expected, is well-predicted by the Euler model.
The drag coefficient was evaluated for the presented geometry (fig 1). The presence of a vertical end of the body made the Euler simulation impossible: in reality, a recirculation zone would take place in the rear flow (downstream to the rocket), so that non-physical points appear in computational domain, making the simulation diverge. Indeed, such a zone cannot be described by an inviscid model. In order to solve this, two configurations were considered: one had an inflow at the vertical end while the other one had a different geometry with an inclined end (*wedge*). Only the second configuration is reported here.
As said before, in the first part of the project simulations are carried out using the Euler equations.

4. Theoretical results

For the validation of the simulation results with the theoretical ones (as concerns the Euler equations), which will be done in section 7, a Matlab program has been developed: receiving in input the Mach, the temperature and the pressure, the program is able to compute the variables of interest on the surface. In order to do it, the program computes the thermodynamic quantities in the free stream, then, knowing the angle of our particular geometry, it calculates the Mach after the first shock using the oblique shock relations. The results after the first shock are then used as input for the expansion that occurs after the second angle. Knowing the sequence of oblique shocks - expansions (and their angles) of our problem, it's then possible to compute the Mach and pressure in all the zones of the surface. In the vertical segment that closes the surface, $p_\infty = 16580\ Pa$ has been used for reasons that will be explained in section 5.1. Multiplying the pressure of each segment by the length of it and taking the horizontal component, is then possible to get the drag force acting on the rocket.
To non-dimensionalize the C_D, a surface of S = π 1.5^2 has been chosen, which is the maximum frontal surface of the rocket. The results are reported in the fig 2.

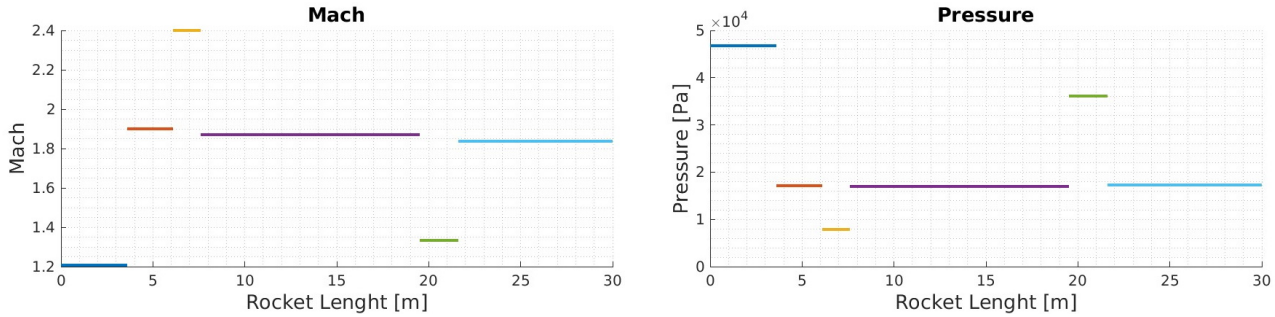

Figure 2: Theoretical Results

$C_D = 0.1629$
Drag = 52943.899 N

To obtain those results the following hypothesis are taken into account: the fluid considered is air (as an ideal gas), with $\gamma = 1.4$ and the flow is inviscid.
Those results are taken as reference for the following paragraphs.

4.1. Boundary conditions

Different boundary conditions were employed for the structured and unstructured grids in the Euler simulations. For the structured one a rectangular domain was considered, while for the unstructured one a semi-circular domain was chosen. This topological difference allowed us to examine the same problems with two sets of boundary conditions in the computational domain. See tab 4.1, fig 3 and fig 4.

	Strucured	Unstructured
Inlet	left wall (supersonic)	x
Outlet	right wall (supersonic)	x
Symmetry	lower wall	lower wall
Farfield	upper wall	upper circular wall
Slip cond.	body	body

5. Grid generation

Both the structured and the unstructured grid involve half of the launcher body, with a symmetry along its longitudinal axis.
A mesh convergence study was lead for each mesh type, to verify the independence of the results from the grid refinement level. In order to do so, we needed first to find the regions that influence the drag the most.

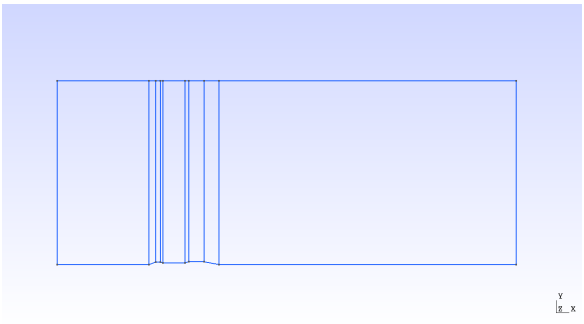

Figure 3: Rectangular domain for the structured grid

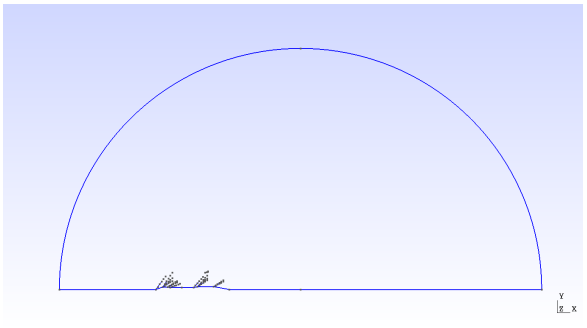

Figure 4: Semi-circular domain of the unstructured grid

While a structured grid allows a more uniform distribution of the cells size, the unstructured one allows more local, discontinuity-tailored refinement.

5.1. Unstructured

The unstructured grid was based on the refinement of the shocks and expansion fans. To do so, the theoretical value of the shock inclinations and fan characteristics were needed. For the shocks a compact refinement was applied along the discontinuity line, while for the expansions the middle characteristic was refined. The length and width of the refinement regions was increased until the pressure at the surface changed over an arbitrary threshold. A slim refinement along the shocks and a short, wide one for the expansions are obtained.

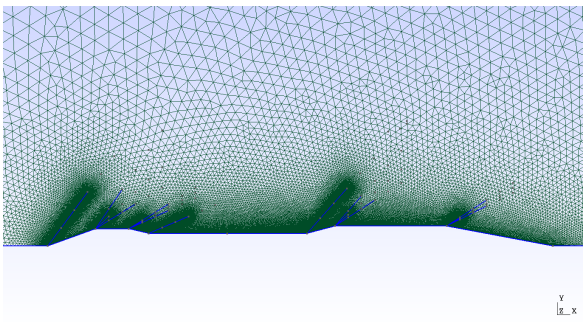

Figure 5: Mesh around the surface

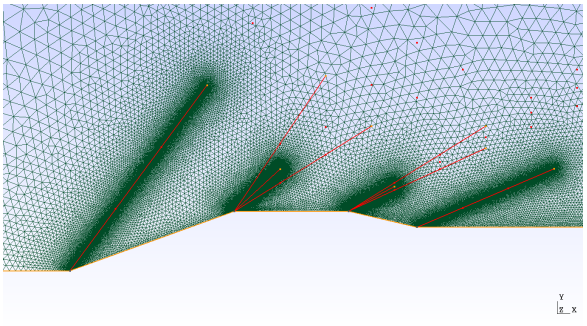

Figure 6: Refinements are slim at the shocks, wide and short at the fans

The domain has a radius $R = 125m$, while the rocket is $38m$ long (the additional $8m$ are given by the rear wedge). No particular refinement is needed behind the body, since we had no interest for the wake development, and so a large grid is used there. The same applies to the elements in front of and above the body, which size is controlled only at the surface: a refinement far from the surface (and from shocks and fans) didn't affect the pressure at the surface. Theoretically speaking, the domain could have been cut with a straight vertical line at the nose to spare some elements (and computational effort), leaving the flow unchanged. Despite that, this simplification was not necessary, given the limited computational effort required for the Euler solution of this case.
For the verification, the grid was refined considering a fixed reduction of the mean size of the elements:

$$\frac{h_{i-1}}{h_i} = 1.35 \tag{1}$$

where the $i-th$ grid element mean size is

$$h_i = \sqrt{\frac{A}{N_i}} \tag{2}$$

where A is the domain area, N_i is the number of elements of the $i-th$ grid. N was increased by refining in the regions that influence the drag: shocks and expansion fans, leaving the farfield elements size unchanged. Five grids where evaluated; the fifth is the finest one. It is apparent how the finest the mesh, the better the capturing of the variables jump (fig 7, 8), since the values become more steady way closer to the discontinuity.

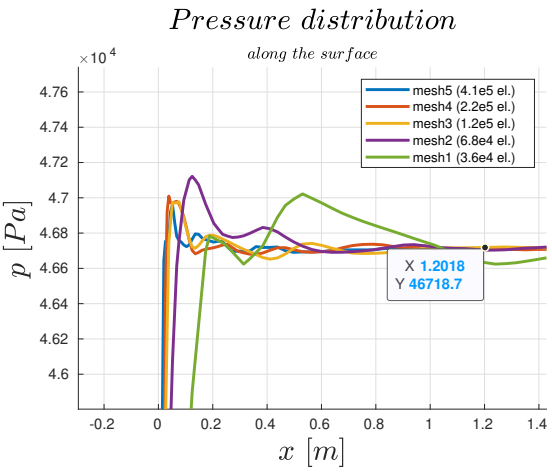

Figure 7: Pressure at the first shock for different meshes

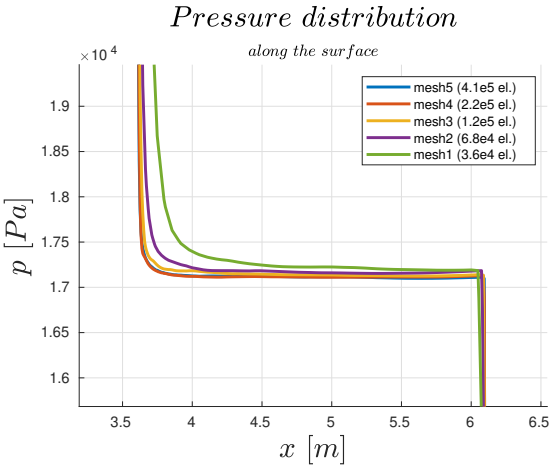

Figure 8: Pressure at the first expansion for different meshes

The fourth grid with $N_4 = 222966$ was chosen, given the small increase at a cost of (almost) doubling the elements (fig. 11): the corresponding drag coefficient is $C_D = 0.19567$. The theoretical one is obtained integrating the surface pressure (from oblique shock relations and Ptrandtl-Meyer expansion) along the surface, giving a $C_D = 0.196192$ (the wedge surface is taken into account). A further confirmation was sought considering the relative error of the surface pressure between the different grids with respect to the finest one. To do so, it was first necessary to have the same number of nodes along the surface for each grid, and so an interpolation was needed (*interp1* function on Matlab [4]). Then, the $norm-2$ error was computed, and compared to the relative error of the C_D with respect to the finest grid. The trend is confirmed, and so the fourth mesh can be used (fig. 12).

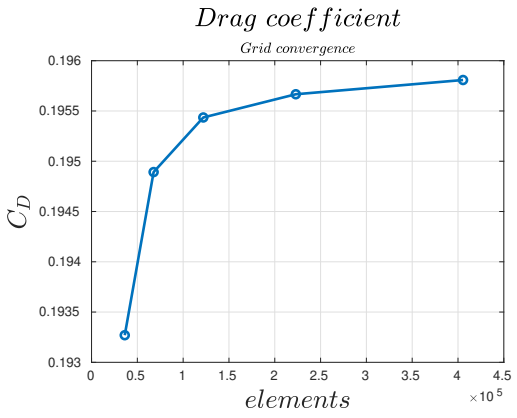

Figure 9: C_D convergence

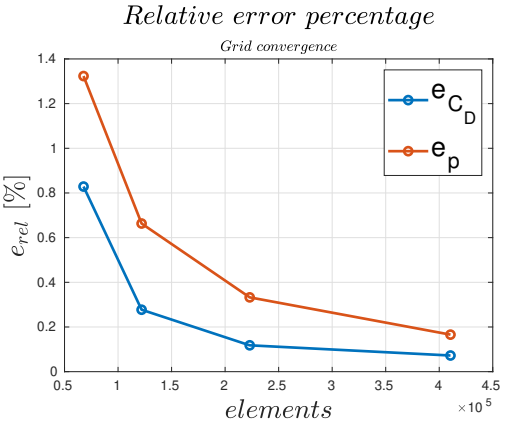

Figure 10: Relative error on the different grids for C_D and p

Though we are aware of the fact the C_D has to be computed in a closed geometry, we decided to exclude the final wedge from its calculation in the following simulations. Considering the simulation with the fourth grid, this gave a lower drag coefficient, of 0.16273. If we computed an integration of the pressure on the surface (but excluding the final wedge) and we make it dimensionless in order to obtain a coefficient similar to the C_D, we would obtain $C_D = 0.2395$. A possible explaining hypothesis is that, being the C_D usually computed on a closed surface, the software integrates (for

the calculation of the drag coefficient) also the freestream pressure along the final height of 1.5 m (i.e. the height of the wedge) equal to 16580 Pa. By computing this "new" C_D by hand, we retrieve $C_D = 0.1629$, which is in agreement with the results obtained with the above-mentioned simulation. A further confirmation of this hypothesis is given by the results obtained in section 8.2, in which the CD is plotted for different Mach numbers (considering, in the integration, also the freestream pressure in the virtual vertical wall).

5.2. Structured

As regards the structured grid, the domain is $250m$ long and $100m$ high. Refinements are done, using a progression, both towards the change in the geometry (i.e. where shock waves and the expansion fans generate) and towards the surface of the rocket; the first one is done in order to better capture the changes in the flow variables, while the second one in order to make the simulation more efficient: this way the elements far from the surface, where the flow doesn't change so much and where it's not of great interest, are bigger. Besides, the mesh is done in order to be coarser over the surface of the final wedge, being this one not considered in the computation of the C_D and of the flow variable variations. All of this leads to a great deal of computational savings in terms of time. A comparison between a mesh refined both near the shock waves and near the expansion fans and a mesh refined only near the shock waves was pursued, in order to see if refining near the fans, which leads to a greater computational efforts, is worth in terms of precision of the results, both as regards the variations of the pressure and the other flow variables, like the Mach. It was observed that, by refining towards both the shocks and the expansion fans, there's just a little improvement (due to the fact that the refinement is not exactly done along the expansion fan, as it is possible to do in the unstructured grid) with respect to the theoretical results, e.g. as regards the Mach variation; however, this improvement is so small that doesn't justify the increase on the computational time needed to obtain convergence of the simulation. That's the main reason why, for the structured mesh convergence, we chose to report just the mesh presenting only the shock refinements. The refinement was done in order to have non-elongated and non-skewed elements where sharp changes occur in the geometry to better capture the flow variables gradients.

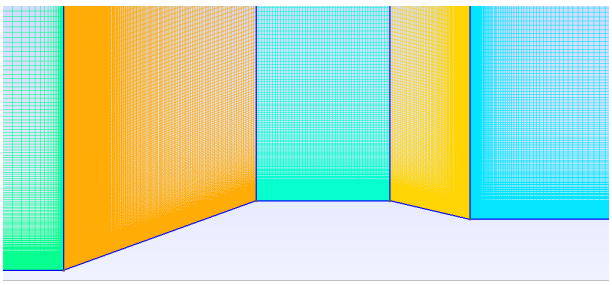

Figure 11: Structured grid with refinements towards the shocks; frontal part of the rocket

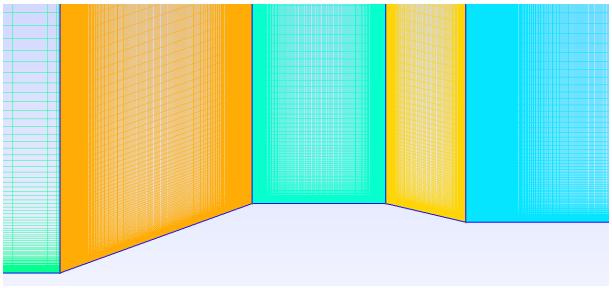

Figure 12: Structured grid with refinements towards shocks and fans; frontal part of the rocket

As said before, a grid convergence study is done for the mesh with refinements only towards the shocks. It was done with respect to the Drag coefficient and also to the pressure value calculated on a large number of points on the surface of the VEGA .

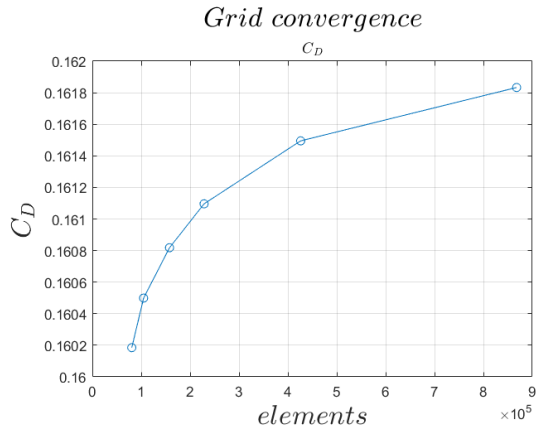

Figure 13: C_D convergence with respect to the number of elements

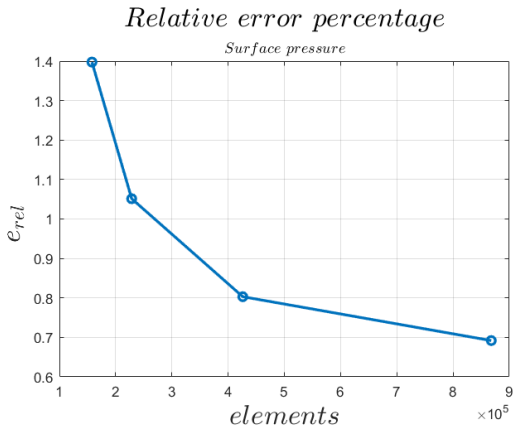

Figure 14: Pressure relative error with respect to the number of elements calculated considering the five most refined meshes

As far as the mesh series is concerned, it consists of six meshes with increasing number of elements, in each of which the ratio between the number transfinite points on the second surface (counting from the nose) and on the vertical lines is always constant. Furthermore, after noticing the importance of elements shape on the refined zones, the ratio between the two dimensions of the final (i.e. the smallest) element of each refine progression is kept constant too.

6. Solver setup

Given the hyperbolicity of the problem, as a numerical scheme, ROE method is used: indeed, this method is an upwind one (a centered scheme, like JST, cannot be used [2]) and it's first order. As a result, the discontinuities, i.e. the shock waves, are smoothed and the flow variables, e.g. the pressure and the Mach, have a substantial difference with respect to the theoretical values. The smoothness is due to the diffusion typical of the first methods. In order to improve these two aspects, the Monotonic Upwind Scheme for Conservation Laws (MUSCL) is used, which, being a high resolution method, retrieves second order accuracy in certain parts of the domain, i.e. where the discontinuities are present. This way the shock waves are sharper and more accurate results in terms of pressure and Mach jumps, for example, are obtained. Also the HLLC scheme was employed, and brought to the same result in a slightly lower number of iterations, yet didn't allow to activate the higher order of the solution.
However, the surface pressure plot shows strong oscillations in correspondence of the discontinuities; these oscillations are expected, indeed second order methods have dispersion problems. In order to attenuate these oscillations, a slope limiter is used; specifically, the Venkatakrishnan-Wang one is used.
The CFL number has been tuned for the two grids to obtain convergence, and to increase its speed: the same problem on the structured grid required a $CFL_{str} = 50$, while on the unstructured a $CFL_{unstr} = 15$.
As convergence criterion we used a convergence on the RMS of the density, set to 10^{-9}.

7. Results

In figure 15 and figure 16, the comparisons for both the pressure and the Mach number between first and second order are reported, as concerns the structured grid (we chose the fourth mesh, with 228545 elements); besides, the theoretical results, also reported in section 4, are plotted; this guarantees the validation of the simulation results for the structure grid, with a maximum error of 1.5% (2.362 instead of the theoretical 2.399), after the second expansion, for what concerns the Mach. This error decreases until under 0.25% after a few centimeters from the surface. This behaviour, i.e. this slight variation of the Mach, is still to be explained; however, it is our purpose to further investigate this phenomenon we have found in the simulations.

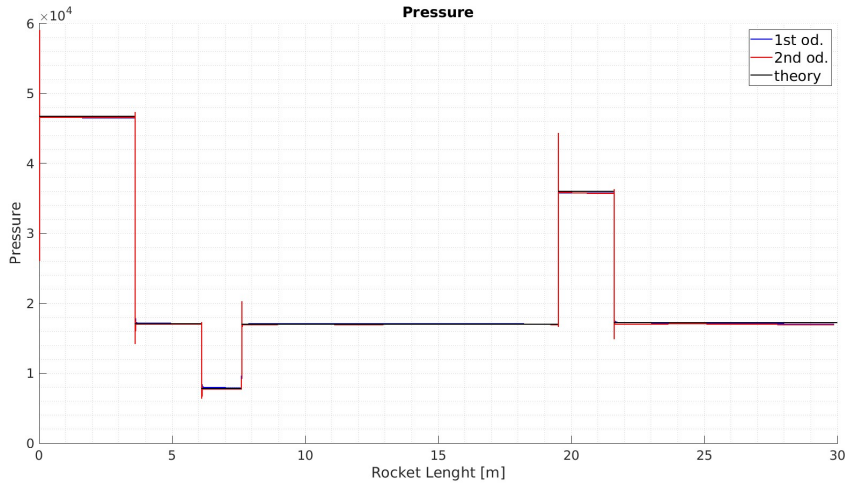

Figure 15: Comparisons of the pressures between first order, second order and the theory results

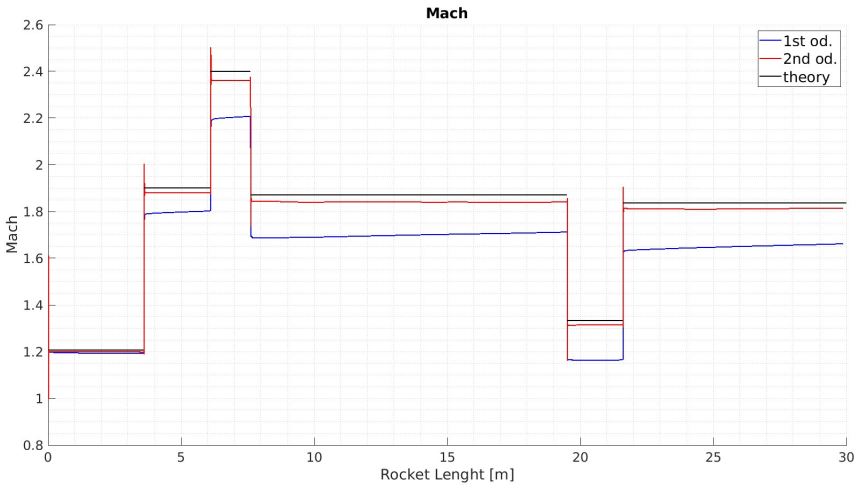

Figure 16: Comparisons of the Mach between first order, second order and the theory results

Looking at the relative error graph (deduced from the surface pressure difference from different meshes similar to each other) in both the structured and the unstructured mesh, it can be noticed the difference of relative error percentage. In fact, the relative error percentage between the last two unstructured meshes is less than 0.2 % whereas in the structured one is near 0.7 %. This result can be explained considering the greater efficiency of the unstructured mesh. In fact, with this type of mesh is possible to refine the elements exactly where is needed while in the structured one is only possible to refine toward a vertical and/or an horizontal transfinite line. This can be seen also from the C_D grid convergence, where is clear that the unstructured mesh reach a higher and more accurate result despite having a lower number of elements. Nevertheless, our structured mesh allows to analyze the problem even in the case of a small change of the boundary conditions whereas in the unstructured one a complete rebuilding of the mesh is needed and this cause a big loss of time. It must be noted that the solution detaches from the theoretical one more an more along the body, especially past the shocks. This is due to an error propagation: each discontinuity generates an error that is accumulated across the flowfield towards the rear part of the body. This is visible in fig 17 and fig 18, where the surface pressure for the unstructured mesh is shown.

A comparison between the structured and unstructured grids is shown in 19, where the pressure is extracted along an horizontal straight line at three distances from the body axis ($1.6m$, $1.8m$, $2.5m$). We focus on the shocks regions because the oscillations at the expansions are less important. It's apparent how the structured solution presents greater oscillations (order of magnitude of $10^3 Pa$ at the first shock) compared to the ones of the unstructured. This behaviour is attributed to the different element sizes: the structured grid elements are smaller, hence give place to higher oscillations (fig 19). Another interesting thing is that the pressure difference between the structured and unstructured solutions remains almost constant at the three heights (fig 20).

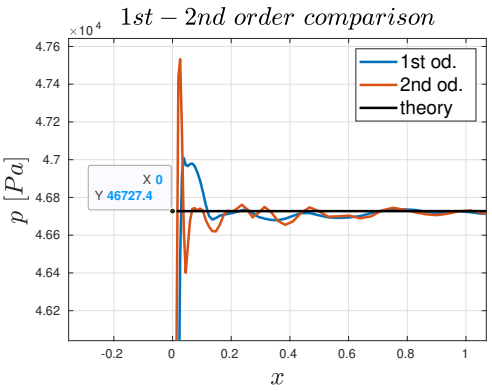

Figure 17: Unstructured: 1st, 2nd order, theory at the first shock

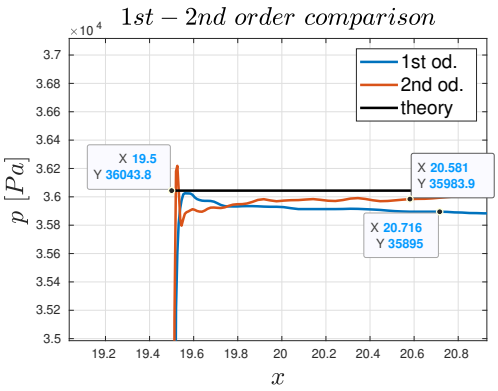

Figure 18: Unstructured: 1st, 2nd order, theory at the third shock

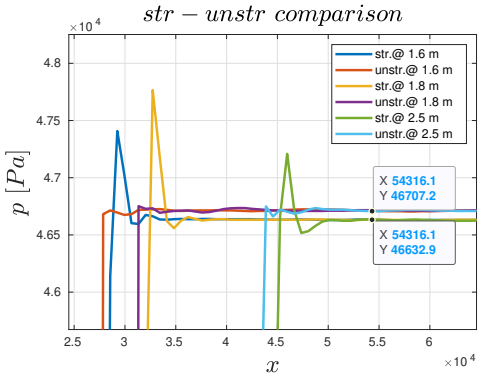

Figure 19: Comparison at different heights, first shock

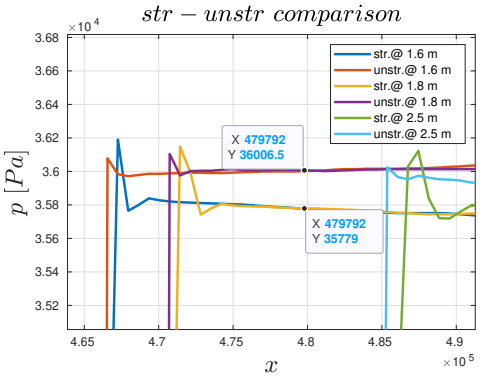

Figure 20: Comparison at different heights, third shock

7.1. Mach variation

The Prandtl – Meyer expansions prescribes a maximum deflection angle that the flow can have for a given Mach. For the description of the rear part of the rocket, a wedge of height 1.5 m and length 8 m is used: in order to check if this approximation can be used without having a detached flow, a small Matlab code was developed. Using a Newton Method, it was found that the maximum Mach in the last horizontal part of the rocket should be less than M = 26.9. This gives us a limit velocity that should not be exceeded while performing the study at different Mach.
Using the tables for the oblique shock relations, it was also observed that the Mach shouldn't be less than M = 1.83 in order to avoid detached shock in the frontal area: this condition would require a different mesh from the one used in our simulations, consequently requiring a major number of nodes in the area before the nose of the rocket. Those two conditions give a range in which the problem can be analyzed with our mesh.

7.2. Problem setup

For this study the structured grid is used, mainly because at the moment when it was performed the structured grid was already checked for mesh convergence. Moreover, the unstructured grid with refinements along the shock lines, that performed very well with fixed Mach, should have been adapted differently for each Mach number, making the use of this specific strategy very time consuming for our goal. Simulations were performed varying the Mach number from M = 1.85 to M = 2.50 with Mach steps of M = 0.05. By using this range we are inside the one above-defined larger safe range. In order to take into account the mesh convergence, a simulation was performed with the mesh with the highest number of elements (with 867917 elements, i.e. the sixth mesh) for M = 2.5, and one with the previous mesh in terms of elements (with 426075 elements, i.e. the fifth mesh), obtaining the following results:

$C_{DFifthMesh} = 0.122596$
$C_{DSixthDetailed} = 0.122869$

% difference = 0.23%

For M = 1.99 the percentage difference between the two mesh is about 0.19%, slightly underestimating the C_D for the lower number-of-element mesh, like for the M = 2.50. Considering what we expect from theory and the results for M = 2.50, that is the maximum Mach used in this section, we hypothesize that the results obtained with the intermediate Mach numbers can be affected by an error of the 5th grid with respect to the 6th less than 0.3%: this assumption allows us to run simulations with good results with the 5th mesh, requiring much less time with respect to the finer mesh, i.e. the 6th.

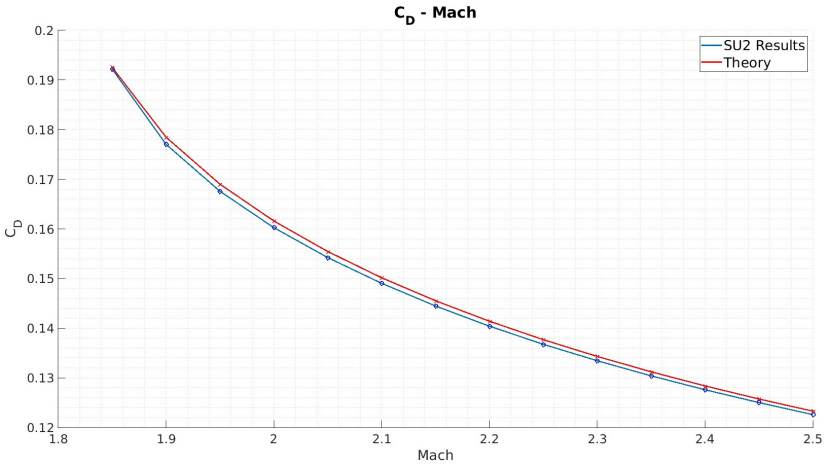

Mach	SU2	Theory	% Diff
1.85	0.19221	0.19254	0.17
1.90	0.17705	0.17848	0.81
1.95	0.16758	0.16901	0.85
2.00	0.16026	0.16160	0.84
2.05	0.15422	0.15545	0.79
2.10	0.14905	0.15016	0.75
2.15	0.14448	0.14553	0.73
2.20	0.14041	0.14140	0.71
2.25	0.13675	0.13769	0.68
2.30	0.13345	0.13431	0.65
2.35	0.13040	0.13122	0.63
2.40	0.12760	0.12837	0.60
2.45	0.12501	0.12574	0.58
2.50	0.12260	0.12329	0.57

In the graph the comparison between the theoretical results, obtained with Matlab, in red, and the SU2 results, in blue, are appreciated. The SU2 simulations predict very well the analytical results, with an error that is always less than 0.85%.
The following picture is a plot of the Mach for the $M_\infty = 1.85$ simulation. The shock is still oblique as predicted by the theory: going with lower Mach we end up in a detached shock, that can't be well captured with the mesh used (showed in the bottom part of the image).

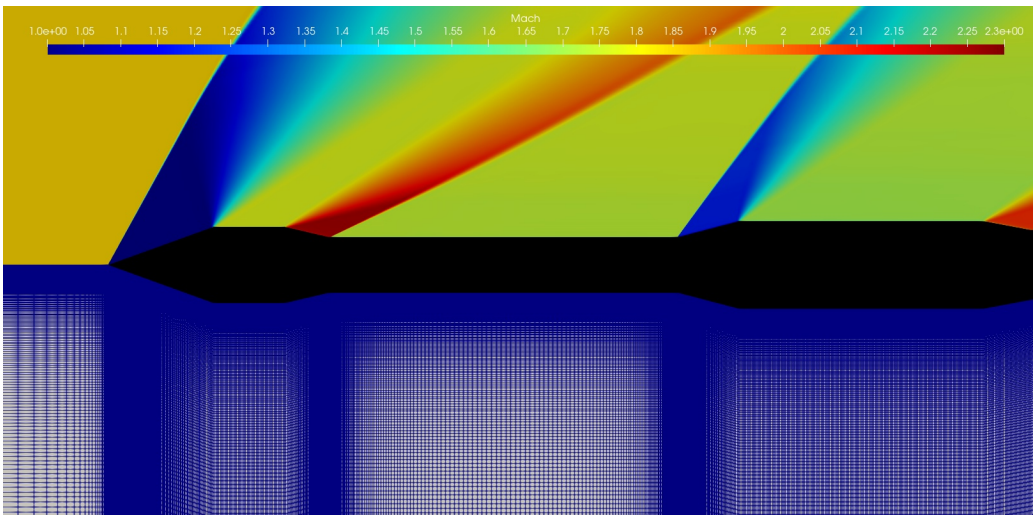

Figure 21: Mach flow visualization for M = 1.85

The percentage difference between theory and SU2 simulation for M = 1.85 is the lowest in the range that is taken into account, with a value of 0.17 %. A possible explanation for this can be that the first and the third shock are more vertical and then better captured by this structured grid, that is more refined in that region.
The figure 22 shows the pressure comparison between the M = 1.85, in the top, and M = 2.50, in the bottom part. The shock angle difference between the two configurations can be appreciated, resulting in a more vertical shock for the M= 1.85.

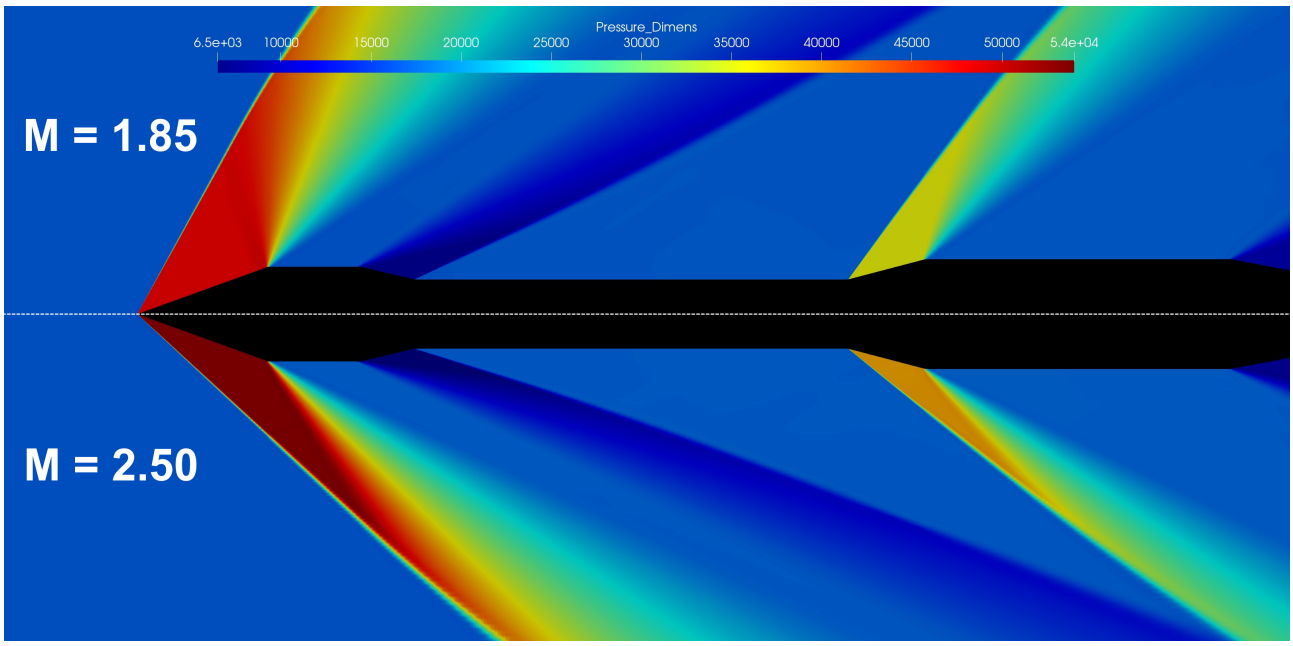

Figure 22: Pressure field comparison between M = 1.85 and M = 2.50

In these simulations only the Mach number has been changed but a future study can also be done changing the pressure and temperature, in order to investigate other flight conditions of the rocket. Furthermore, it has to be said that mesh convergence for each Mach number was not done, for limited time reasons; however, as said before, the obtained results seem in good agreement with the theoretical predictions.

7.3. RANS

As far as Reynolds-Averaged Navier-Stokes' equations are concerned, a completely structured grid has been analyzed. In this case study, it has been necessary to create a structured grid near the wall, and that is mainly because of two reasons: y+ $<$ 1 and the need to study the characteristics of the homogeneous flow in that particular region. The y+ is the wall distance made dimensionless with the viscous length δ_ν which is the ratio between the cinematic viscosity ν and the friction velocity u_ν; instead the friction velocity is given by the square root of the ratio between the wall stress τ_w and density ρ. The equations are reported here [6]:

$$\begin{aligned} \delta_\nu &= \frac{\nu}{u_\nu} \\ u_\nu &= \sqrt{\frac{\tau_w}{\rho}} \\ y^+ &= \frac{y}{\delta_\nu} \end{aligned}$$

Hence, it's important to refine the mesh in order to get a small-enough cell next to the wall in a way to correctly capture the viscous effects. This means that the first cell height is equal-or-less with respect to the viscous length. In the structured grid, it is obtained the following diagram for y+:

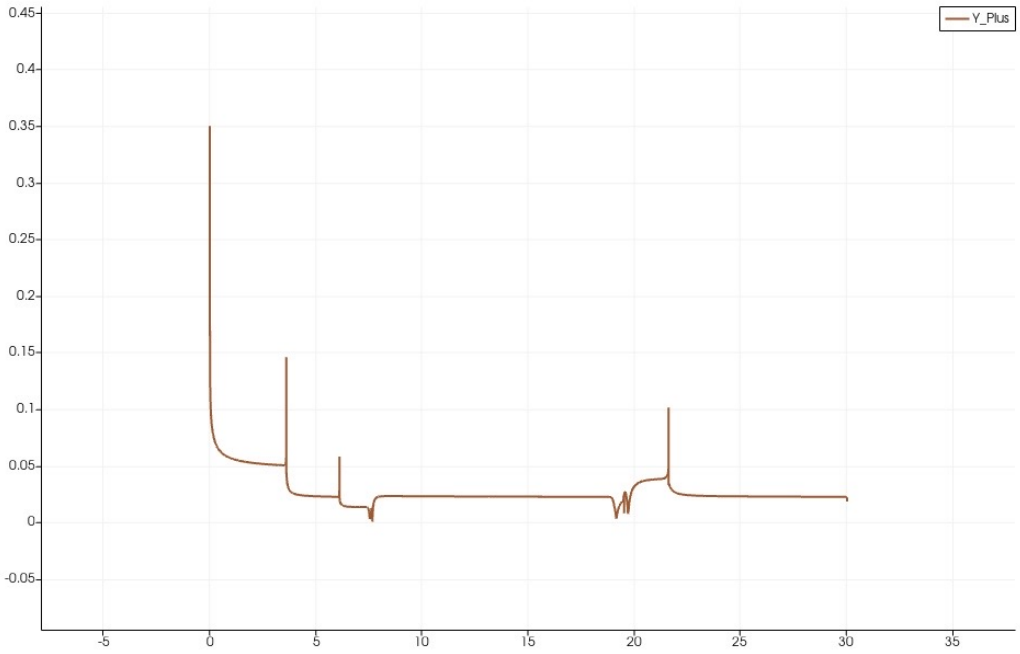

Figure 23: y+ for structured grid

As far as the turbulence model is concerned, the SST model was used instead of the SA one, and that is because the latter is an one-equation model and because of that it may present the following problems:

− SA model is optimised for transonic flows, and the study is supersonic (Mach = 1.99).

− It is known that SA model doesn't work well in case of flows with adverse pressure gradients.

The SST turbulence model is a two-equation model, and because of that it overcame these problems and seemed adequate to the study. In the numerical configuration a turbulence intensity of 0.01 was used, considering an altitude of 13000 m. For the numerical method, ROE scheme seemed the most accurate considering that the rocket is travelling at supersonic speed; that's because it is an upwind numerical method. Furthermore, the MUSCL option was added in order to better capture the solutions near the discontinuity zones of the flow field (as shock waves and rarefaction fans) like in the Euler equations problem seen before [2]. In addition to that, the surface pressure plot doesn't present oscillations near the point in which the field present those discontinuities, and that's thought to be because of the dissipation terms present in RANS equations. It is reported the Mach comparison between the first order and second order:

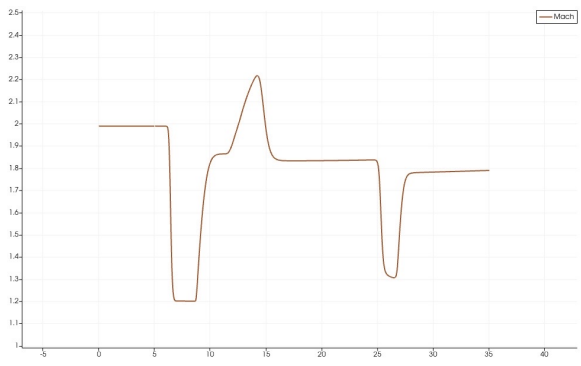

Figure 24: Mach with ROE

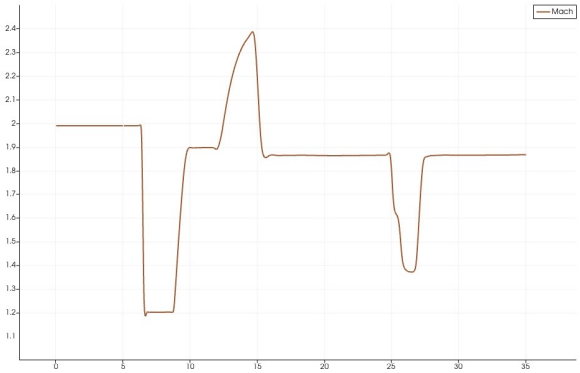

Figure 25: Mach with ROE + MUSCL

As said before, the solution with MUSCL presents oscillation but they are more damped than Euler case for the viscosity presents in RANS equation.

8. Axialsymmetry

Simulations with axialsymmetry were done with Euler and RANS equations to further approach the *real* case. In this case, it is not possible to make the complete theoretic validation for time absence, but it could be a proposal for future developments.

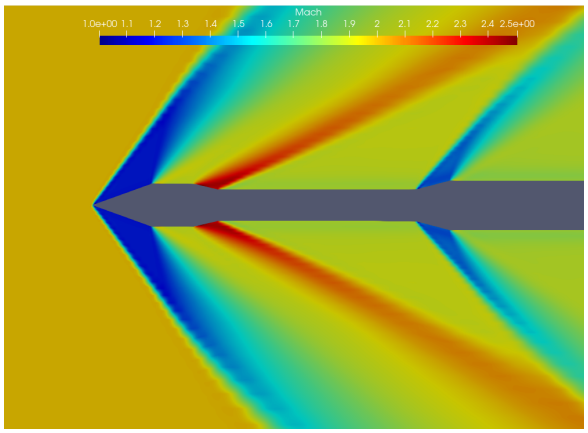

Figure 26: Mach with Euler

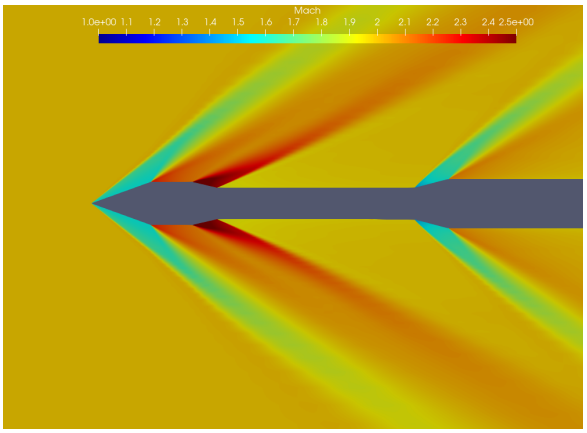

Figure 27: Mach with axialsymmetry Euler

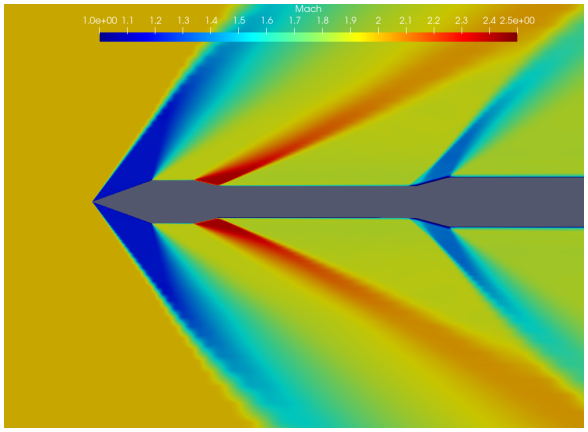

Figure 28: Mach with RANS

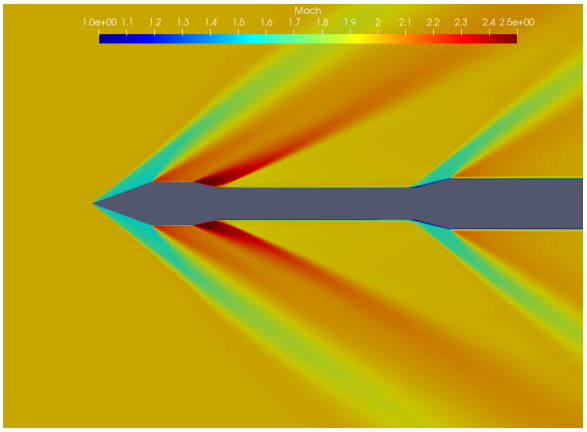

Figure 29: Mach with axialsymmetry RANS

It can be seen how the shock-waves present a slightly smaller angle with respect to the inclined surface compared to the two-dimensional case. This fact can be explained taking into account the Taylor-Maccoll theory for conical shock waves from which the governing differential equation of the flow around the cone can be derived. The 'new' angle can be computed using a diagram obtained by the numerical resolution of the governing differential equation [3]:

$$\frac{1}{c}\cdot\frac{d^2u}{d\theta^2}\left(\frac{\gamma+1}{2c^2}\left(\frac{du}{d\theta}\right)^2-\frac{\gamma-1}{2}\left(1-\frac{u^2}{c^2}\right)\right)=(\gamma-1)\frac{u}{c}\left(1-\frac{u^2}{c^2}\right)$$
$$+\frac{\gamma-1}{2c}\cdot\left(1-\frac{u^2}{c^2}\right)\cot\theta\cdot\frac{du}{d\theta}-\frac{\gamma u}{c^3}\left(\frac{du}{d\theta}\right)^2-\frac{\gamma-1}{2c^3}\cot\theta\left(\frac{du}{d\theta}\right)^3$$

Figure 30: u and v are the radial and and tangential components of velocity of the air in the region between the solid cone and the conical shock wave. The angle of the component u w.r.t. the x axis is named theta.

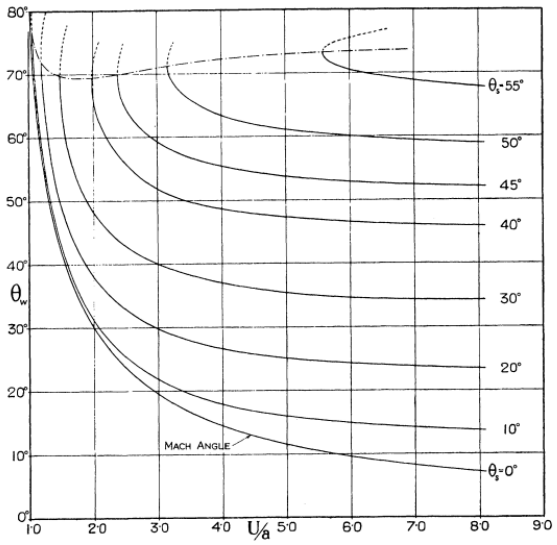

Figure 31: Maccoll diagram with iso-cone-angle lines.

Comparing the image and the diagram above, it can be seen the similarity of the results obtained; in fact, the exact wave angle is 37.821° while the value in the simulation is approximately 38°, as far as the first shock is concerned. As said before, we didn't perform further analysis because of lack of time.

9. Conclusions

The project goal was to study the C_D and pressure distribution over the simplified rocket surface, while trying to obtain the best possible results at the lowest computational cost. In order to achieve it, different meshes are used with different advantages and disadvantages. A valid example could be the two types of meshes used in the Euler study: the complete structured and the unstructured one. In this particular case, it is seen that if more precise results are desired, unstructured mesh is needed. Nevertheless, in this case the refinement along all the shock waves is required and it is possible to do it only if it is known the solution in advance. Instead, if more freedom of changing the boundary conditions of the study while maintaining the same mesh is preferred, in this case it's better to choose the structured one. Also in the viscous study a structured grid is chosen in order to achieve a better ductility. As future development, it could be interesting to use an hybrid mesh, hence structured in the boundary layer and unstructured outside. All the results obtained have been validated with the theory, so it is possible to conclude that the the numerical analysis is reliable. Nonetheless, it has to be said that the results obtained could be slightly improved with a larger number of elements but it wasn't done in this study both for lack of time and the excessive computational costs.

References

[1] J.D. Anderson. *Fundamentals of Aerodynamics.* McGraw-Hill Education, 2010.

[2] Randall J. LeVeque. *Numerical Methods for Conservation Laws.* Birkhauser, 1992.

[3] J. W. Maccoll. *The Conical Shock Wave formed by a Cone moving at a High Speed.* Royal Society, 1936.

[4] MATLAB. *version 9.13.0.2049777 (R2022b).* The MathWorks Inc., Natick, Massachusetts, 2022.

[5] ESA Media Relations Office. Vega qualification flight vv01. *The name of the journal*, page 13, 2012.

[6] Stephen B. Pope. *Turbulent Flows.* Cambridge University, 2000.